Scripta Materialia 278 (2026) 117262

Contents lists available at ScienceDirect

Scripta Materialia

journal homepage: www.journals.elsevier.com/scripta-materialia

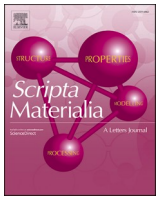

On the precipitability of binary Ti alloys bearing 4-period *d*-metal eutectoid stabilisers

L. Bolzoni *, F. Yang

School of Engineering, The University of Waikato, Hamilton 3240, New Zealand

ARTICLE INFO

Keywords:
Titanium alloys
Eutectoid transformation
Phase diagram
Electronic structure
Molybdenum equivalent parameter

ABSTRACT

There is no specific, simple approach for predicting whether the addition of an eutectoid beta stabiliser to Ti leads to an 'active' eutectoid transformation upon primary processing (e.g., sintering). Here, we demonstrate that, among theoretical/empirical models, phase diagram features, and electronic structure parameters, the hypoeutectoid area is the best predictor, followed by the molybdenum equivalent parameter (MoE), of the precipitability for 4-period *d*-metals. As the area increases, which corresponds to the addition of progressively stronger β-eutectoid stabilisers, the less active the eutectoid phase transformation, changing from pearlitic to bainitic (i.e., need for an ageing heat treatment). This occurs if the MoE weighted coefficient is, respectively, lower than or higher than 1. This is because molybdenum is taken as reference, and the higher the coefficient, the larger the drop of the β transus temperature (i.e., higher stabilisation). Valid for 4-period *d*-metals, it remains to be proven for 5-period and 6-period *d*-metals.

The development of Ti alloys for high demanding engineering applications relies on the addition of specific alloying elements, which are commonly divided between α and β stabilisers. The latter are further divided between isomorphous and eutectoid depending on the resulting phase diagram [1]. β-eutectoid stabilisers are desirable because they are the strongest stabilisers and they are generally cheaper than Ti, which is beneficial in the quest to reduce the cost of Ti alloys [2]. However, the addition of β-eutectoid stabilisers can lead to the precipitation of brittle intermediate phases. This can either be appositely targeted to enhance specific performance, for instance mechanical properties [3] or antibacterial capability [4], or it can be an unwanted side effect of the incorporation of a specific alloying element in the chemical composition. When intermediate phases are desired, they are generally achieved by means of a precipitation hardening heat treatment (i.e., solid solution plus ageing) similarly to Al-, Ni- and Mg-based alloys amongst others [5], although precipitation upon primary processing (i.e., pearlitic from near-equilibrium cooling conditions) also occurs. When intermediate phases are unsought, careful selection of the elements is crucial. Nevertheless, due to the complexity of the associated eutectoid reaction (which is pearlitic/bainitic in nature in many systems), the problem has been overlooked in literature, and a simple guiding relationship is not available. Specifically, cooling rate, eutectoid temperature and composition, martensitic transformation start temperature, and diffusivity [6] are all meant to affect the eutectoid precipitation, and so are the electronic structure and the reaction kinetics. Most of these features (e.g., eutectoid point) vary broadly in Ti alloys bearing 4-period *d*-metal, making them ideal to tackle the issue. Therefore, the objective of this work is to revisit the eutectoid precipitation in binary Ti alloys, identify key aspects that promote/hinder the formation of intermediate phases, and provide a framework for choosing alloying elements based on the desired outcome (e.g., presence of precipitated intermediate phases, equivalent to an active eutectoid phase transformation upon primary processing). Specifically, the eutectoid transformation behaviour was methodically analysed against available theories (e.g., molybdenum equivalent), phase diagram features (e.g., eutectoid point), and parameters of the electronic structure (e.g., electron affinity). It is worth mentioning that the work focuses on hypoeutectoid and near-eutectoid compositions where the nucleation and growth of the 'first' intermediate phase occurs via an invariant eutectoid transformation.

Generally, the addition of an eutectoid stabiliser to Ti reduces the allotropic phase transformation temperature (i.e., β transus) and introduces either a monotectoid or an eutectoid phase transformation [7]. Specifically, the ability to stabilise the β phase can be defined by the slope of the β transus and the extend of α solubility, which decreases for more potent β stabilisers. 4-period *d*-metal eutectoid stabilisers span from Cr (group 6, BCC), to Co (group 9, HCP), and to Zn (group 12, FCC),

* Corresponding author.
E-mail address: bolzoni.leandro@gmail.com (L. Bolzoni).

https://doi.org/10.1016/j.scriptamat.2026.117262
Received 16 December 2025; Received in revised form 9 February 2026; Accepted 2 March 2026
Available online 6 March 2026

with all of them resulting in the occurrence of an eutectoid transformation with the exception of Cr (Fig. 1). Due to its characteristic monotectoid transformation, Cr is the only element with a 'first' intermediate phase with TiM_2 structure (i.e., $TiCr_2$), which switches to TiM (i.e., Mn and Fe) and eventually to Ti_2M (where M is a generic d-metal) as the group number increases where electronegativity, valency, and relative atomic size determine the structure of the intermediate phase. Temporarily disregarding Zn due to its remarkably lower melting point (Supplementary Table 1), Cr is also the only element that do not fit the increasing invariant eutectoid transformation temperature (i.e., Mn→Cu) with the increase of the 4-period d-metal group number as its transformation temperature (i.e., 667 °C) its higher than that of Mn (i.e., 550 °C). Generally, the combination of high eutectoid composition and low eutectoid temperature (i.e., strong β stabilisation) results in a less active eutectoid transformation.

Starting from the pioneering work of Franti et al. [8], who analysed the eutectoid decomposition of ten binary Ti alloys systems, a significant amount of experimental research has been done on the pearlitic/bainitic transformation in Ti alloys to understand its nature [6], mechanisms [9], interphase boundary structures [10], and morphology/crystallography [11]. As summarised in Fig. 2, the key findings are that in both hypo-eutectoid and near-eutectoid binary Ti alloys systems, the TTT curve shifts towards lower temperatures and longer times (from seconds to weeks) with the decrease of the group number (i.e., Cu→Mn). This is corroborated by the XRD patterns of the sintered hypoeutectoid Ti-2.5Cu alloy and aged hypoeutectoid Ti-5Mn alloys. The Ti_2Cu intermediate phase readily precipitates at the allotropic α/β interphase boundaries upon crossing the eutectoid temperature during slow cooling from sintering. Conversely, the TiMn intermediate phase was not detected after an ageing heat treatment. Specifically, the binary alloys were made via the blended elemental powder metallurgy approach, using commercially available powders including a hydride-dehydride Ti powder (particle size lower than 75 μm, irregular morphology, oxygen 0.28 wt. %, Goodfellow UK), an electrolytic Cu powder (particle size lower than 45 μm, dendritic morphology, purity of 99.7 %, Merck KGaA Germany), and a comminuted Mn powder (particle size lower than 63 μm, irregular morphology, purity of 99.0 %, Sigma-Aldrich USA). The correct amount of elemental powders were mixed in a V-blender 30 min using a speed of 30 rpm prior to their cold uniaxial pressing at 600 MPa, and vacuum sintering at 1250 °C for 2 h with a heating and cooling rate of 10 °C/min (i.e., near-equilibrium). The heat treatment procedure included a solution treatment in the β region at 900 °C for 5 h before water quenching, followed by ageing at 400 °C for 24 h with natural cooling to room temperature as designed on the basis of supporting studies [12,13]. As a longer eutectoid decomposition time is needed (i.e., much lower rate of intermediate phase nucleation), the phase transformation transitions from pearlitic (i.e., P – lamellar eutectoid decomposition entailing the ledge-controlled, cooperative growth of two phases) to bainitic (i.e., B – non-lamellar, ledge-controlled, competitive eutectoid decomposition where the two phases nucleate and grow non cooperatively) with the pearlitic transformation only active in Cu due to its high diffusivity and relatively low melting point (Supplementary Table 1). In hypoeutectoid alloys, eutectoid α is sympathetically nucleated, with a slight misorientation (i.e., partially coherent), at the interphase boundaries of proeutectoid α and so is the precipitation of the intermediate phase. This leads to the typical plate morphology developed epitaxially from the morphology of proeutectoid α plates [9]. Pronouncedly elongated (Fig. 2d) or roughly equiaxed intermediate phase crystals will precipitate depending on whether the growth ledge height (h) to average spacing between ledge (λ) ratio of eutectoid α and of the intermediate phase are, respectively, comparable (i.e., pearlitic) or significantly different (i.e., bainitic). As this difference increases, one phase overgrows the other, forcing the latter to repeatedly re-nucleate, forming essentially independent nucleated intermediate phase crystals [10].

The molecular orbital model [14] and the molybdenum equivalent parameter are two theoretical/empirical frameworks commonly used to develop Ti alloys. The former is based on two alloying parameters: the bond order ($\overline{B_o}$), which measures the strength of the covalent bond between atoms, and d orbital energy level ($\overline{M_d}$), which accounts for the hybridisation of the d orbitals, as defined in Fig. 3. The values of both $\overline{B_o}$ and $\overline{M_d}$ for 4-period d-metal eutectoid stabilisers decrease as the group number increases (i.e., Cr→Cu) leading to the associated change of the stoichiometric ratio of the precipitable intermediate phase (i.e., TiM_2→Ti_2M). As the increase of the group number carries a change of the intrinsic lattice of the alloying element (Fig. 1a) so changes the crystalline structure of the intermediate phase. Precisely, Cr leads to an intermediate phase with hexagonal crystal structure, Mn and Fe to BCC, Co and Ni to FCC, and Cu and Zn to tetragonal. This means that, in the case of the 4-period d-metal eutectoid stabilisers, when elements with a BCC lattice (Fig. 1) are added to Ti, the stoichiometry of the intermediate phase determines its crystal structure; conversely, the addition of elements with a room temperature FCC/HCP lattice results in the precipitation of an intermediate phase with Ti_2M stoichiometry, whose crystal structure transitions from FCC to tetragonal as the 4-period d-metal group number increases. The molybdenum equivalent parameter takes into account the relative stabilisation strength of alloying elements used in Ti as compared to molybdenum where, at least, five different definitions (Fig. 3d) are available in literature [15–19]. These definitions were developed based on aspects such as the minimum concentration of

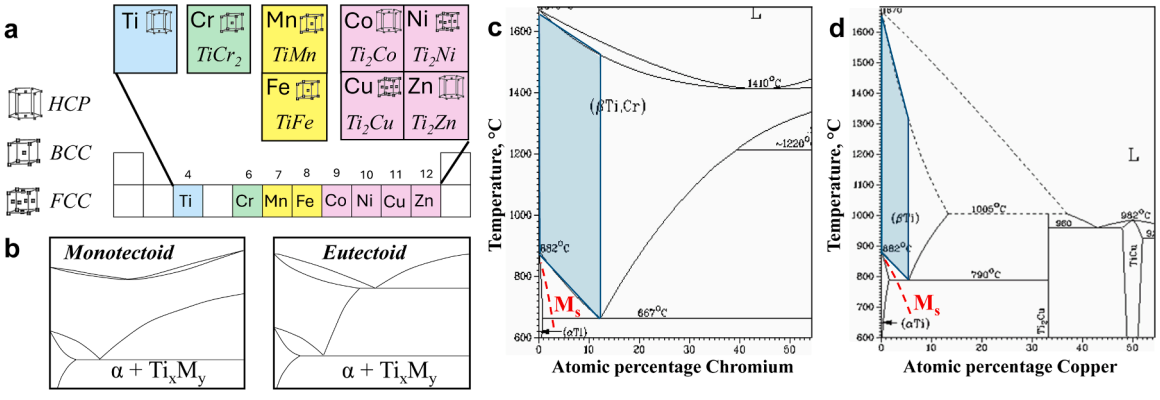

Fig. 1. Details of the 4-period d-metal eutectoid stabilisers considered: a) sketch of the relevant portion of the periodic table showing the elements position, their room temperature stable crystalline structure, and the 'first' intermediate phase found in the respective binary phase diagram when alloyed to Ti, b) sketch of the outcome of the addition of 4-period d-metal in Ti resulting in a binary diagram with an invariant monotectoid/eutectoid transformation, and c-d) Ti-rich portion of the Ti-Cr and Ti-Cu binary phase diagrams, respectively, showing the corresponding monotectoid/eutectoid phase transformation (the shaded area highlights the effect of the element on the stabilisation of the allotropic β phase, the martensite start temperature M_s is sketched as dashed line).

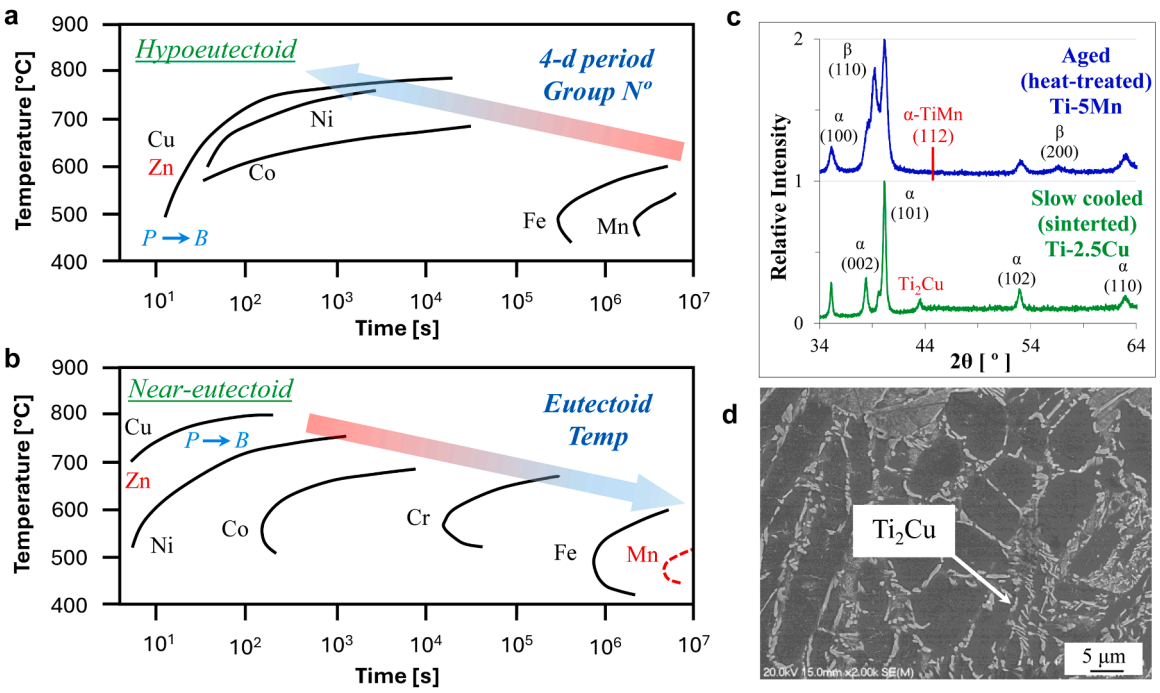

Fig. 2. Precipitation behaviour of binary Ti alloys bearing 4-period *d*-metal eutectoid stabilisers (*P* and *B*, respectively, strands for pearlitic and bainitic): a) TTT diagram for hypoeutectoid compositions (adapted from [8]), b) TTT diagram for near-eutectoid compositions (adapted from [8], note: for the sake of simplicity, the Mn curve was estimated based on its relative position to the Fe curve in hypoeutectoid alloys), c) XRD patterns of the sintered hypoeutectoid Ti-2.5Cu alloy and heat-treated (i.e., solution plus ageing) hypoeutectoid Ti-5Mn alloy, and d) high magnification scanning electron micrograph showing the elongated morphology (i.e., $h_{\alpha\text{-}Ti}/\lambda_{\alpha\text{-}Ti} \approx h_{Ti2Cu}/\lambda_{Ti2Cu}$) of the readily precipitated Ti_2Cu intermediate phase formed upon slow cooling after sintering.

alloying elements needed to obtain a fully stable β microstructure upon quenching or the slope of the β transus temperature (i.e., border line between the single phase β field and the two-phase α+β region). This resulted in equations having different weighted coefficients for the same element with, generally, [19] having the lowest values and [18] the highest. However, broadly, the lower the weighted coefficient of an element (which roughly decreases with the increase of the group number, with once again Cr being the exception) the higher the likelihood of directly precipitating the intermediate phase upon primary processing (i.e., more active eutectoid transformation). This, concurrently, means higher changes of the eutectoid reaction being pearlitic rather than bainitic. For the 4-period *d*-metal eutectoid stabilisers this, approximately, occurs when the weighted coefficient is lower than 1, and more so the leaner the composition, provided it is higher than the α solubility. It is worth noting that, although both theoretical frameworks are commonly used to design new Ti alloys, the molybdenum equivalent parameter is more widely used due to its simplicity [20].

The precipitability of the 4-period *d*-metal eutectoid stabilisers was calculated as the average time in seconds for the precipitation of the intermediate phase in hypoeutectoid and near-eutectoid alloys as per their TTT curves of Fig. 2. Those values were correlated with the theoretical/empirical models previously described (Fig. 3), parameters of the binary phase diagram related to the eutectoid phase transformation, and pertinent aspects of the electronic structure of the 4-period *d*-metal eutectoid stabilisers analysed. The full list of parameters and their values are available in the Supplementary Table 2. It is worth mentioning both the data of the molecular orbital model and the different molybdenum equivalent parameter equations all refer to how the addition of the 4-period *d*-metal eutectoid stabilisers determine the stabilisation of the allotropic β phase. Coherently, during the analysis of the binary phase diagrams [7], the effect of the elements on stabilising the β phase was accounted for by quantifying the corresponding hypoeutectoid area in the diagrams, as exemplified by the shaded areas highlighted in the representative binary diagrams with an invariant monotectoid/eutectoid transformation (Fig. 1c-d). The results of the logarithmic Spearman's rank correlation are shown in Fig. 4 comparing the correlations in the case when Zn is, respectively, excluded or included as some of the data for Zn had to be estimated or calculated due to the fact that the addition of Zn to Ti has been far less studied with respect to the others 4-period *d*-metal eutectoid stabilisers. In particular, due to its high diffusivity and low melting point that results in a active eutectoid reaction able to form pearlite [21] (i.e., lamellar eutectoid decomposition with the cooperative growth of elongated intermediate phase crystals, $h_{\alpha\text{-}Ti}/\lambda_{\alpha\text{-}Ti} \approx h_{Ti2Zn}/\lambda_{Ti2Zn}$), the precipitability of Zn was set to be equal to that of Cu to have a more comprehensive understanding of the effect of all 4-period *d*-metals. Furthermore, $\overline{B_o}$ for Zn is not available in literature and could not be estimated (as $\overline{B_o}$ was found to be more relevant than $\overline{M_d}$) and, therefore, was not considered during the analysis. The molybdenum equivalent parameter for Zn, which is not empirically available as it requires a dedicated systematic quenching study, was calculated using the slope of the β transus temperature as per [18] (see supplementary info), using the binary Ti-Zn phase diagram [22].

It is found that when Zn is excluded from the analysis (Fig. 4a), the precipitability strongly correlates with all the phase diagram parameters analysed as well as with the electron affinity of the 4-period *d*-metal eutectoid stabilisers. Apart from other more expected relationships (e.g., eutectoid temperature and composition), because of their relations with the precipitability, the parameters of the phase diagrams are, therefore, also related to the electron affinity. Overall, this results in 20 % of the logarithmic Spearman's rank correlations being considered significant (i.e., > 0.91). Of the five molybdenum equivalent parameter equations analysed, for which the results of the best two are presented in Fig. 4 for the sake of simplicity, it is found that the equation put forward by Dobromyslov and Elkin [19] is the best to predict the precipitability. The exclusion of Mn, whose TTT curve for near-eutectoid alloys was estimated (Fig. 2b), does not radically change the nature of the correlations, though it makes the Dobromyslov and Elkin's molybdenum equivalent

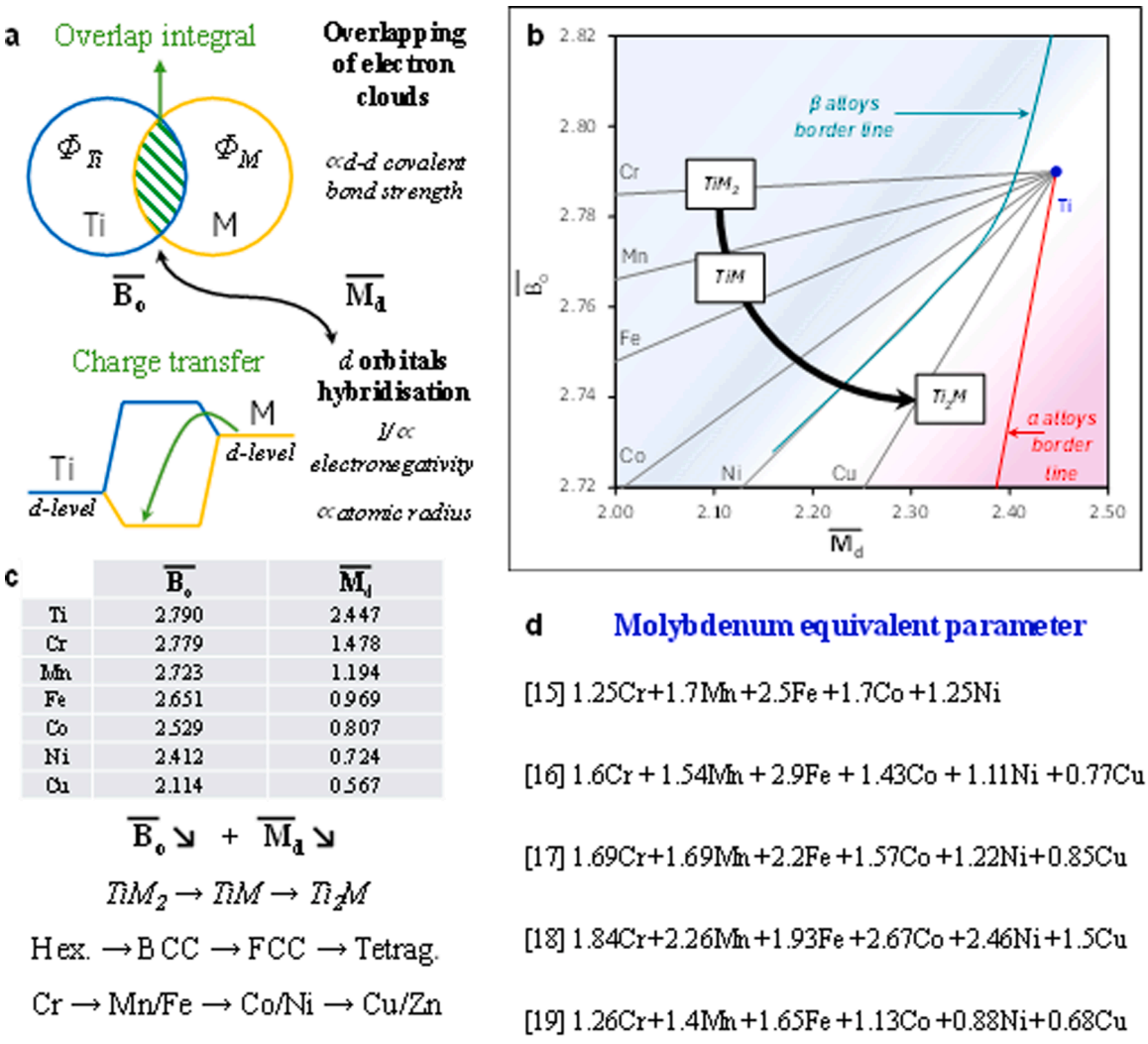

	$\overline{B_o}$	$\overline{M_d}$
Ti	2.790	2.447
Cr	2.779	1.478
Mn	2.723	1.194
Fe	2.651	0.969
Co	2.529	0.807
Ni	2.412	0.724
Cu	2.114	0.567

$\overline{B_o}\searrow + \overline{M_d}\searrow$

$TiM_2 \rightarrow TiM \rightarrow Ti_2M$

Hex. → BCC → FCC → Tetrag.

Cr → Mn/Fe → Co/Ni → Cu/Zn

Fig. 3. Theoretical/empirical models commonly used to develop Ti alloys: a) definition of the alloying parameters of the molecular orbital model [14] – bond order ($\overline{B_o}$) and *d* orbital energy level ($\overline{M_d}$), b) $\overline{B_o}$ – $\overline{M_d}$ map showing the effect of 4-period *d*-metal eutectoid stabilisers on the phase stability of Ti, c) $\overline{B_o}$ and $\overline{M_d}$ values and their effect on the stoichiometry and crystalline structure of the intermediate phase, and d) molybdenum equivalent parameter equations.

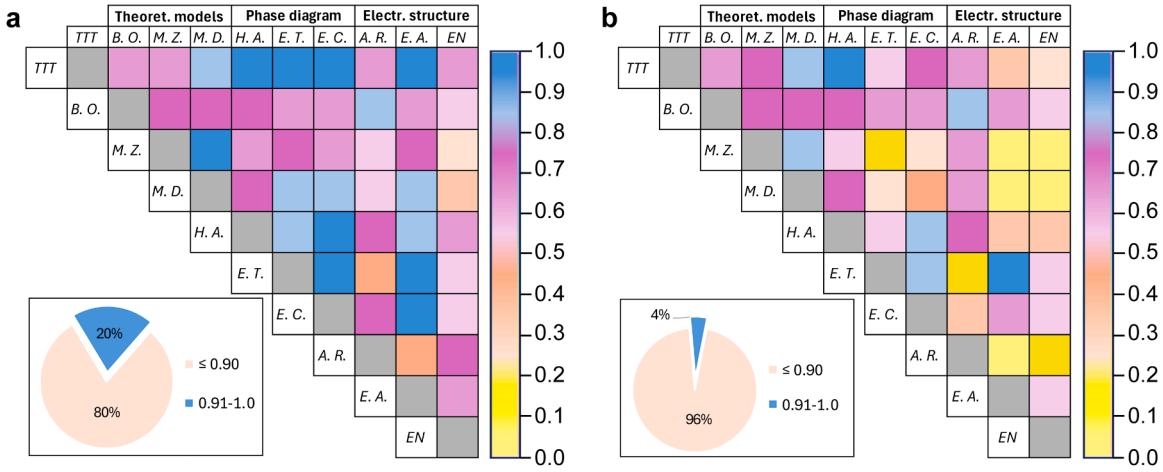

Fig. 4. Logarithmic Spearman's rank correlation showing the strength of the relationship between precipitability (Fig. 2) and relevant parameters: a) Spearman's heat map excluding Zn, and b) Spearman's heat map including Zn. Legend: *TTT* – time for precipitating the intermediate phase as estimated from the TTT curves of Fig. 2, *B. O.* – bond order ($\overline{B_o}$) parameter of the molecular orbital model, *M. Z.* – molybdenum equivalent parameter as proposed by Zhou [17], *M. D.* – molybdenum equivalent parameter as proposed by Dobromyslov and Elkin [19], *H. A.* – hypoeutectoid area of binary phase diagrams [7] (examples are shown in Fig. 1c-d as shaded areas), *E. T.* – eutectoid temperature, *E. C.* – eutectoid composition, *A. R.* – atomic radius, *E. A.* – electron affinity, and *EN* – electronegativity.

parameter [19] significant (Supplementary Fig. 1). Generally, the inclusion of Zn in the analysis (Fig. 4b) significantly worsen the correlations between the precipitability and the parameters analysed as well as the relationships amongst the distinct aspects considered, with only 4 % of the logarithmic Spearman's rank correlations being significant. Notwithstanding of the limitations for the need to estimate some data (especially for Zn), it holds true that the eutectoid temperature is related to the electron affinity, but more importantly, that the overall precipitability trend of the 4-period *d*-metal eutectoid stabilisers is best predicted through the simple quantification of the hypoeutectoid area of the respective binary phase diagram [7]. Reiterating, this is because the hypoeutectoid area accounts for the global effect that each individual 4-period *d*-metal eutectoid stabiliser has on the equilibrium phase diagram as well as possible metastable phase transformations (e.g., martensite and omega, though the latter has been far less studied using eutectoid stabilisers in comparison to isomorphous beta stabilisers like Mo and V). For instance, the martensite start temperature (Fig. 1c-d) initially shifts towards lower (Cr→Fe) and subsequently towards higher (Co→Cu) temperatures with the addition of 4-period *d*-metal eutectoid stabilisers [6]. If, for the sake of simplicity, the molybdenum equivalent parameter wants to be utilised, than Dobromyslov and Elkin's equation [19] should be used. Elements with a lower weighted coefficient, especially if lower than 1, will be more prone to precipitate an intermediate phase and, preferentially, lead to a pearlitic eutectoid phase transformation (i.e., active) entailing the formation of lamellar grains with cooperatively nucleated and grown α and Ti_2M crystals upon primary processing. It is worth noting that the effect of the β-eutectoid stabilisers on the precipitability is absolute, not subtractive/cumulative. For instance, the eutectoid phase transformation will be active (i.e., pearlitic) if both a high group number (i.e., weak β-eutectoid stabiliser like Cu) and a low group number (i.e., strong β-eutectoid stabiliser like Mn) 4-period *d*-metal eutectoid stabilisers are concurrently added; even when the latter has a higher proportion than the former (e.g., Ti-5Mn-2.5Cu) [23]. This does not necessarily mean that the simultaneous addition of different 4-period *d*-metal eutectoid stabilisers will not affect the morphology of the precipitated intermediate phase crystals.

Data availability

All metadata pertaining to this work will be made available on request.

CRediT authorship contribution statement

L. Bolzoni: Methodology, Investigation, Conceptualization. **F. Yang:** Methodology.

Declaration of competing interest

The authors declare that they have no known competing financial interests or personal relationships that could have appeared to influence the work reported in this paper.

Acknowledgements

This research did not receive any specific grant from funding agencies in the public, commercial, or non-profit sectors.

Supplementary materials

Supplementary material associated with this article can be found, in the online version, at doi:10.1016/j.scriptamat.2026.117262.

References

[1] R. Boyer, G. Welsch, E.W. Collings, Materials Properties Handbook: Titanium Alloys, in: A. International (Ed.) Ohio, USA, 1998.
[2] L. Bolzoni, M. Paul, F. Yang, Effect of combined lean additions of isomorphous and eutectoid beta stabilisers on the properties of titanium, J. Mater. Res. Technol. 21 (2022) 3828–3843.
[3] N. Yumak, K. Aslantaş, A review on heat treatment efficiency in metastable β titanium alloys: the role of treatment process and parameters, J. Mater. Res. Technol. 9 (6) (2020) 15360–15380.
[4] E. Zhang, X. Zhao, J. Hu, R. Wang, S. Fu, G. Qin, Antibacterial metals and alloys for potential biomedical implants, Bioact. Mater. 6 (8) (2021) 2569–2612.
[5] S. Kirklin, J.E. Saal, V.I. Hegde, C. Wolverton, High-throughput computational search for strengthening precipitates in alloys, Acta Mater. 102 (2016) 125–135.
[6] A.V. Dobromyslov, Bainitic transformations in titanium alloys, Phys. Met. Metallogr. 122 (3) (2021) 237–265.
[7] J.L. Murray, Phase diagrams of binary titanium alloys, 1st ed., ASM International, 1987.
[8] G.W. Franti, J.C. Williams, H.I. Aaronson, A survey of eutectoid decomposition in ten Ti-X systems, Metall. Trans. A 9 (11) (1978) 1641–1649.
[9] H.J. Lee, H.I. Aaronson, Eutectoid decomposition mechanisms in hypoeutectoid Ti-X alloys, J. Mater. Sci. 23 (1) (1988) 150–160.
[10] T. Furuhara, H.J. Lee, E.S.K. Menon, H.I. Aaronson, Interphase boundary structures associated with diffusional phase transformations in Ti-base alloys, Metall. Trans. A 21 (6) (1990) 1627–1643.
[11] T.A. Bhaskaran, R.V. Krishnan, S. Ranganathan, On the decomposition of β phase in some rapidly quenched titanium-eutectoid alloys, Metall. Mater. Trans. A 26 (6) (1995) 1367–1377.
[12] E. Zhang, J. Ren, S. Li, L. Yang, G. Qin, Optimization of mechanical properties, biocorrosion properties and antibacterial properties of As-cast Ti-Cu alloys, Biomed. Mater. 11 (6) (2016) 065001.
[13] M. Ikeda, M. Ueda, R. Matsunaga, M. Ogawa, M. Niinomi, Isothermal aging behavior of beta titanium-manganese alloys, Mater. Trans. 50 (12) (2009) 2737–2743.
[14] M. Morinaga, Alloy design based on molecular orbital method, Mater. Trans. 57 (3) (2016) 213–226.
[15] K. Molchanova, Phase diagrams of titanium alloys, translation of atlas diagram sostoyaniya titanovyk splavov), Israel Program for Scientific Translations, Jerusalem, 1965, p. 154.
[16] P.J. Bania, Beta titanium alloys and their role in the titanium industry, JOM 46 (7) (1994) 16–19.
[17] Y.B. Zhou, Titanium alloy casting, Aviation Industry Press, Beijing, China, 2000.
[18] Q. Wang, C. Dong, P.K. Liaw, Structural stabilities of β-Ti alloys studied using a new Mo equivalent derived from [β/(α + β)] phase-boundary slopes, Metall. Mater. Trans. A 46 (8) (2015) 3440–3447.
[19] A.V. Dobromyslov, V.A. Elkin, Martensitic transformation and metastable β-phase in binary titanium alloys with d-metals of 4-6 periods, Scr. Mater. 44 (6) (2001) 905–910.
[20] M. Alqattan, Y. Alshammari, F. Yang, L. Peters, L. Bolzoni, Biomedical Ti-Cu-Mn alloys with antibacterial capability, J. Mater. Res. Technol. 10 (2021) 1020–1028.
[21] D.A. Brice, P. Samimi, I. Ghamarian, Y. Liu, M.Y. Mendoza, M.J. Kenney, R. F. Reidy, M. Garcia-Avila, P.C. Collins, On the eutectoid transformation behavior of the Ti-Zn system and its metastable phases, J. Alloys. Compd. 718 (2017) 22–27.
[22] H. Okamoto, Ti-Zn (Titanium-Zinc), J. Ph. Equilibria Diffus. 29 (2) (2008) 211–212.
[23] M. Alqattan, L. Peters, Y. Alshammari, F. Yang, L. Bolzoni, Antibacterial Ti-Mn-Cu alloys for biomedical applications, Regen. Biomater. 8 (1) (2020) rbaa050.